Pang, J.; Wischke, C.; Lendlein, A.:
**In vitro Degradation Analysis of 3D-architectured Gelatin-based Hydrogels.**
In: MRS Advances . Vol. 5 (2020) 12 - 13, 633-642.
First published online by Cambridge University Press: 28.11.2019

DOI: 10.1557/adv.2019.441
https://dx.doi.org/10.1557/adv.2019.441

# *In vitro* Degradation Analysis of 3D-architectured Gelatin-based Hydrogels

Jun Hon Pang[1], Christian Wischke[1], Andreas Lendlein[1,2,*]

[1]Institute of Biomaterial Science and Berlin-Brandenburg Center for Regenerative Therapies, Helmholtz-Zentrum Geesthacht, Teltow, Germany.
[2]Institute of Chemistry, University of Potsdam, Potsdam, Germany
*Correspondence to: Andreas Lendlein
E-mail: andreas.lendlein@hzg.de

ABSTRACT

Multifunctional biopolymer-based materials are promising candidates for next generation regenerative biomaterials. Understanding the degradation behavior of biomaterials is vital for ensuring biological safety, as well as for better control of degradation properties based on rational design of a material's physical and chemical characteristics. In this study, we decipher the degradation of a hydrogel prepared from gelatin and lysine diisocyanate ethyl ester (LDI) using in vitro models, which simulate hydrolytic, oxidative and enzymatic degradation (collagenase). Gravimetrical, morphological, mechanical and chemical properties were evaluated. Notably, the hydrogels were relatively resistant to hydrolytic degradation, but degraded rapidly within 21 days (>95% mass loss) under oxidative and collagenase degradation. Oxidative and collagenase degradation rapidly decreased the storage and loss modulus of the hydrogels, and slightly increased their viscous component (tan δ). For each degradation condition, the results suggest different possible degradation pathways associated to the gelatin polypeptide backbone, urea linkages and ester groups. The primary degradation mechanisms for the investigated gelatin based hydrogels are oxidative and enzymatic in nature. The relative hydrolytic stability of the hydrogels should ensure minimal degradation during storage and handling prior to application in surgical theatres.

## INTRODUCTION

Pure biomaterials-based strategies combining important biochemical and physical cues to direct tissue regeneration *in vivo* are highly desirable in regenerative medicine[1, 2]. Multifunctional materials capable of providing the sophisticated microenvironment and mimicking the native extracellular matrix are required for such therapeutic approaches [3]. Specific protein presentation, tailorable structural function, pore morphology, and controlled degradability are some vital factors to consider. However, for translation into clinical applications, a balance between complexity and engineering simplicity needs to be considered. This supports the use of biopolymers with

capacity for cell/tissue compatibility and adjustment of their properties and functions by chemical and/or physical approaches as needed.

Hydrogels remain a vital pillar of biomaterials for regenerative therapies due to their high biomimicry of physical properties with regard to native soft tissues [4]. Gelatin, in particular, when compared to other natural biopolymers such as collagen, is of low immunogenicity, relatively inexpensive, and provides the key active biological sequence to promote cell integration [5]. Targeted towards clinical translation of a regenerative biomaterial implant, we developed a multifunctional 3D-architectured gelatin-based hydrogel, formed through a one-pot synthesis by reacting gelatin with lysine diisocyanate ethyl ester (LDI). These structured hydrogels exhibit essential properties and functions at different hierarchical levels including tunable degradability and elastic properties, dimensional stability upon swelling, an interconnected porous architecture, and presentation of cell adhesive sequences [6]. The use of LDI ensures non-cytotoxic amino acid-based degradation components [7]. *In vivo* studies in rats and mice have demonstrated promise in promoting, for example, bone regeneration [8]. While it is known that these hydrogels are degradable *in vivo*, there is limited understanding of the contribution of different degradation mechanisms.

Probing degradation mechanisms of medical device candidates is vital for the assessment of biological safety. The *in vivo* environment is complex and animal studies may not necessarily translate directly to patients. The main *in vivo* degradation pathways include hydrolytic, oxidative, and enzymatic degradation. In *in vitro* experiments, these degradation pathways can be simulated [9]. Hydrolytic degradation refers to chemical attack of polymer chains by water molecules and is most notable on ester bonds but may occur on amide bonds present in gelatin backbone, at lower rates, at least at neutral pH. Oxidative degradation is typically mediated by reactive oxygen species (ROS), which are secreted by cells such as macrophages, endothelial cells or foreign body giant cells. ROS can initiate the oxidation process by abstraction of hydrogen atoms on α-methylene groups of the polymer. Further radical-radical reactions then lead to either crosslinking, or intermediate formation of hemiacetal which subsequently result in chain scission [10]. Ether linkages are especially known to be prone to such oxidative degradation, producing carboxyl and hydroxyl terminated chains, while ester bonds tend to be relatively resistant against oxidative degradation [11, 12]. Oxidative degradation could also occur in urethane and possibly urea bonds, albeit to a lesser extent [13, 14]. Enzymatic degradation, which could be challenging to accurately model *in vitro* due to the plethora of enzymes present *in vivo* at different times and locations, is mainly attributed to accelerated hydrolysis of specific chemical bonds by aid of biocatalyst(s) [15].

In this study, we investigate the fate of gelatin-based hydrogels *in vitro* under degradation conditions simulating pure hydrolysis, enzyme catalyzed hydrolysis and oxidative stress conditions. The degradation rates as well as changes in porous structure, rheological properties and chemical functional groups are evaluated. Due to the gelatin and lysine based composition of the hydrogel, we hypothesize that the hydrogel is prone to oxidative and enzymatic degradation, but should be relatively resistant to hydrolytic degradation.

## EXPERIMENTAL

### Preparation of hydrogels

Architectured hydrogels were synthesized as previously reported [6]. 10% (w/v) aqueous gelatin solution (gelatin porcine skin, 200 bloom, type A, low endotoxin content, GELITA, Iowa, USA) was reacted in presence of 1% (w/v) poly(ethyleneglycol)-*block*-

poly(propyleneglycol)-*block*-poly(ethyleneglycol) (Pluronic F-108, Sigma Aldrich, Steinheim, Germany) with LDI (Chemos GmbH, Altdorf, Germany) at 8-fold molar excess of isocyanate groups compared to $NH_2$ groups of gelatin. For removal of unreacted components, the material was immersed and washed in water. The produced hydrogels were freeze dried and sterilized prior to use.

**Degradation experiment**

Each sample (dimensions: 15 × 15 × 3.5 $mm^3$) was immersed in 5 mL of their respective test solutions in 50 mL centrifuge tubes, and were incubated at a standing position at 37 °C with gentle agitation of 60 rpm in an incubator (Certomat IS, Sartorius Stedim Biotech GmbH, Göttingen, Germany). The following test solution conditions and their respective buffer compositions were used: (i) hydrolytic degradation condition, 10 mM phosphate buffer saline (PBS), pH 7.4; (ii) oxidative degradation condition, 3% (v/v) $H_2O_2$ (Sigma Aldrich, Steinheim, Germany) in deionized water (DI $H_2O$); (iii) enzymatic degradation condition, 0.2 U/mL Collagenase I (Gibco, Life Technologies, New York, USA) in 10 mM PBS, pH 7.4. Each solution was supplemented with 0.01% (w/v) sodium azide (Merck KGaA, Darmstadt, Germany). Degradation media change was conducted regularly every 3-4 days. At each time point, samples were retrieved from their degradation media using a sieve with pore size of 40 µm (Falcon cell strainer, Corning, New York, USA), and were frozen at -30 °C for a minimum of 1 day, and subsequently freeze-dried over a period of 3 days (Christ Alpha 2-4 LSC, Martin Christ GmbH, Osterode, Germany).

**Characterization of hydrogels**

The initial dry mass of each sample was measured with a weighing balance (XP205 Delta Range, Mettler Toledo, Giessen, Germany). At each time point, freeze-dried samples from each condition (n = 6) were retrieved as described above. The final dry mass was measured, and the percentage of mass loss was determined according to the following formula, where $m_i$ is the initial dry mass, $m_t$ is the dry mass as the respective time point:

$$Relative\ mass\ loss\ (\%) = \frac{m_i - m_t}{m_i} \times 100\%$$

The surface morphology of the freeze-dried samples were analyzed by scanning electron microscopy (SEM) using a Phenom G2 pro SEM (Phenom-World, Darmstadt, Germany) after conductive coating deposition in the form of a thin gold layer (~5 nm thick) using a sputter coater (Polaron, Quorum Technologies Ltd, Lewes, UK).

The storage modulus (G') and loss modulus (G") of swollen hydrogels were determined by rheology using HAAKE MARS III rheometer (Thermo Fischer Scientific, Reichenthal, Germany). Freeze-dried samples of ~3.5 mm thickness and ~19 mm diameter were prepared with a stainless steel cylindrical puncher, and were incubated in their respective degradation media (n = 5) as described above under 'degradation experiment'. Samples were retrieved after 1, 4 and 7 days, rinsed with distilled water, and were freeze-dried prior to characterization. Samples were incubated overnight in 10 mM PBS (pH 7.4, Gibco, Life Technologies, New York, USA) at 37 °C under mild shaking. Measurements were performed at 37 °C using a 20 mm plate-plate measurement geometry, with a constant shear stress of 4 Pa and a constant oscillation frequency of 1 Hz for 180 s. To account for the varying thicknesses of samples over degradation, the plate-to-plate distance for each sample was set when a stable normal force of 0.3 ± 0.03 N was attained. The plate-to-plate distance ranged from 3.8 mm for non-degraded samples to 0.25 mm for degraded samples at later time points.

Attenuated total reflectance Fourier-transform infrared spectroscopy (ATR-FTIR) was applied on freeze-dried samples after incubation in the degradation conditions described above using a Nicolet 6700 FTIR (Thermo Fisher Scientific, Waltham, USA) spectrometer. Spectra were collected by averaging 50 scans at a resolution of 4 $cm^{-1}$.

### Statistical analysis

Data reported are expressed as mean ± standard deviation (SD). Statistical analysis was performed using Prism v5 (GraphPad, San Diego, USA) with two-way analysis of variance (ANOVA) followed by Bonferroni *post-hoc* test. A *p*-value of $p < 0.05$ was considered statistically significant.

## RESULTS & DISCUSSION

Freeze-dried hydrogels from gelatin and LDI were incubated under conditions simulating hydrolytic, oxidative, and enzymatic degradation. The hydrolytic and oxidative conditions were selected in accordance to ISO 10993-13 [16]. Collagenase was selected for enzymatic degradation conditions, as it is present at the site of implantation, where acute or chronic tissue damage leads to inflammatory states with often high levels of MMPs, including collagenase. Several studies have reported an effect of collagenase on degradation of gelatin-based materials [17, 18]. The addition of 0.01% (w/v) sodium azide into the buffers exclude possibility of microbial contamination effects.

Figure 1 shows the mass loss over time of the hydrogels incubated under the different conditions. The hydrogels degraded rapidly under oxidative and enzymatic degradation, where mass loss was immediately apparent from day 1 (~10% for oxidative and ~15% for enzymatic). 50% mass loss was achieved before day 7, and the hydrogels achieved complete degradation (defined as > 95% mass loss). The degradation rate between oxidative and enzymatic degradation were comparable. In contrast, the hydrogels displayed minimal mass loss up to day 28 against hydrolytic degradation, and appeared relatively stable up to day 140 (~15% mass loss), with subsequent gradual decline to ~34% mass loss recorded after 280 days.

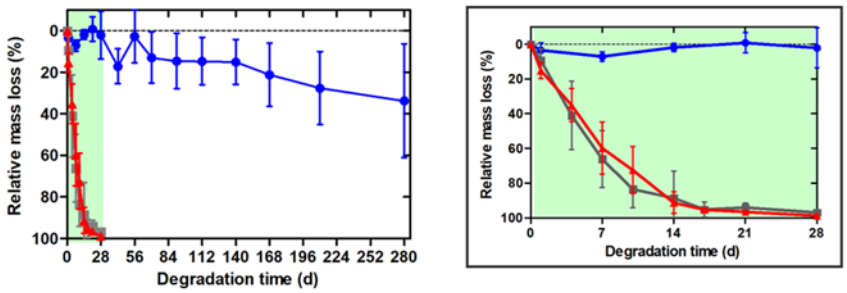


Figure 1: Mass loss of architectured hydrogels under *in vitro* hydrolytic (● in blue), oxidative (■ in grey) and enzymatic (▲ in red) degradation conditions (data expressed as mean ±SD, n = 6). Right graph in box represents an enlargement up to 28 days (area highlighted green).

SEM images of the freeze-dried samples after collection from the degradation buffer confirmed substantial differences for hydrolytic compared to oxidative and

enzymatic degradation (Figure 2). The surface of the hydrogel (untreated) was innately porous. Under hydrolytic degradation, no cracks or fragmentation was observed after 14 days. Oxidative degradation resulted in small surface defects such as cracks already on day 1, although it could be attributed to artifacts from freeze drying. However, successive erosion of the samples were observed on day 7, where the internal open porous structure of the hydrogel could be seen. Enzymatic degradation partially revealed the internal open porous structure on day 1, and increasing sample erosion were resulted in subsequent time points. On day 14 under both oxidative and enzymatic conditions, the hydrogels seemed to have lost their original physical form and structure.

The results from these macroscopic and microscopic evaluation indicated that the gelatin-based hydrogels are relatively resistant against hydrolysis, but are labile in presence of Collagenase I and oxidative agents. Nonetheless, hydrolytic degradation conditions may still change molecular structure and material morphology, which could influence the mechanical properties of hydrogels.

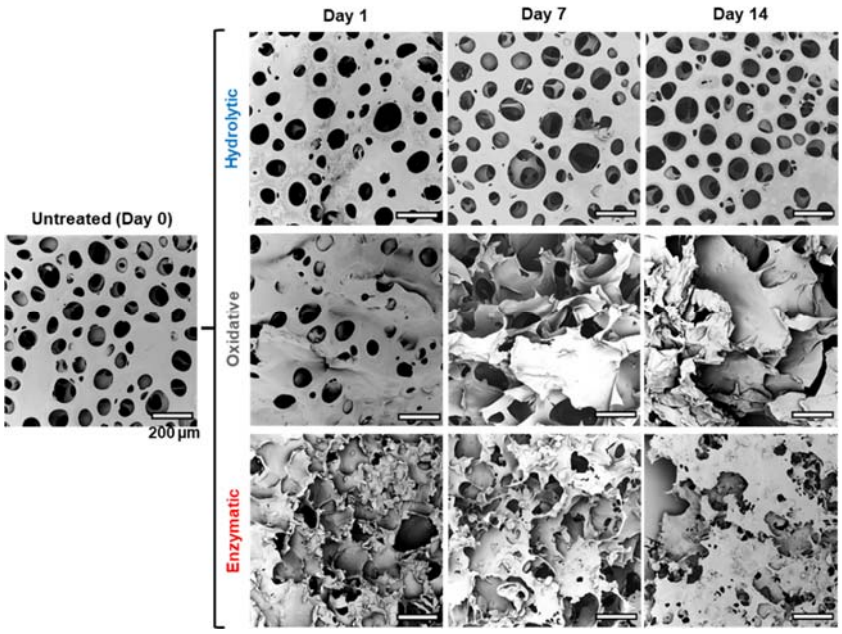


Figure 2: Representative SEM images of untreated and freeze-dried samples collected after incubation in hydrolytic, oxidative and enzymatic conditions for 1, 7 and 14 days. Scale bar = 200 µm.

For hydrogels as viscoelastic materials, rheology is a suitable method to elaborate mechanical features under physiological temperature 37 °C in the hydrated state. The initial G' and G" of untreated hydrogels were in the range of 3687 ± 507 Pa and 162 ± 20 Pa, respectively, which indicates a predominantly elastic behavior. Under hydrolytic degradation, G' decreased slightly (~16% at day 1) but remained fairly constant up to day 7, while G" remained similar to the initial state at all time points of investigation (Figure 3A-B). Oxidative degradation resulted in the highest decrease in both G' and G", with

~97% and ~94% decrease recorded on day 7. Enzymatic degradation resulted in ~82 and ~70% decrease on day 7.

To analyze the relative changes of G' and G", tan δ (i.e. ratio of G" to G') can be calculated to measure viscous properties with respect to elastic properties. The tan δ values among all datasets are considerably low in the range of 0.03-0.09, indicating a predominantly elastic behavior as justified by the covalent network structure of the investigated samples. However, a significant increase in tan δ was clear in the case of oxidative and enzymatic degradation at day 4 and 7 compared to day 1 ($p < 0.05$) (Figure 3C). On day 4 and 7, the increase in tan δ of oxidative degraded samples was significantly higher than enzymatically degraded samples, and enzymatically degraded samples was higher than hydrolytically degraded samples ($p < 0.05$). The results overall infer a decrease in elasticity of the hydrogels, thus it is likely that the covalent network structure is degraded [19, 20]. This could either be cleavage of the gelatin polypeptide backbone, or degradation of the LDI derived urea-based linkages formed through the reaction between isocyanate and amine groups [21].

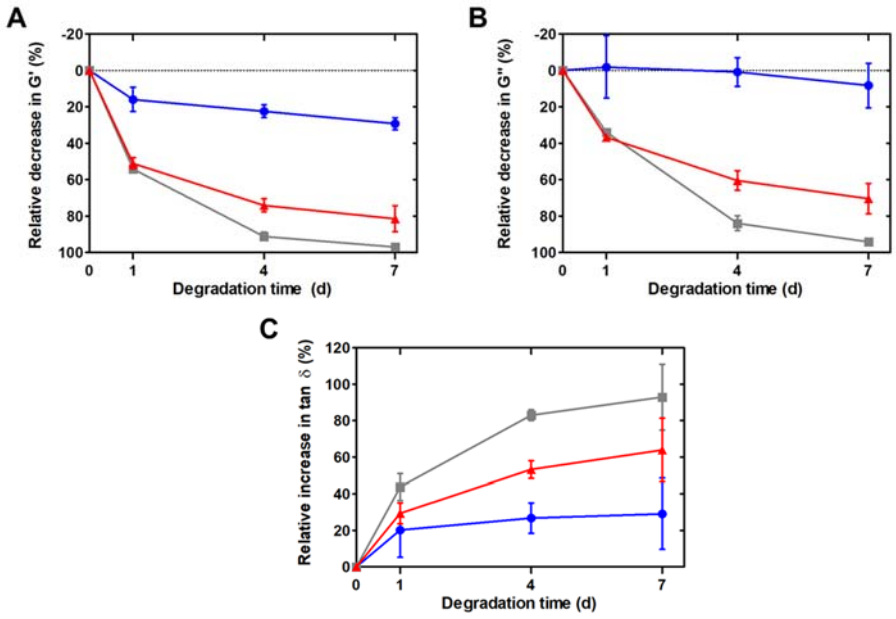


Figure 3: Rheological measurements of hydrated samples after partial degradation in hydrolytic (● in blue), oxidative (■ in gray) and enzymatic (▲ in red) degradation conditions. (A) Relative reduction in storage modulus G' (B) relative reduction in loss modulus G", and (C) relative increase in tan δ in comparison to untreated hydrogels (day 0). Data expressed as mean ± SD (n = 5).

FTIR analysis of the hydrogels after incubation in the respective condition did not show obvious differences up to day 7 (Figure 4). Emergence of an additional peak at 1734 $cm^{-1}$ after oxidation and enzymatic degradation could initially be observed at day 7, but became obvious at day 14. Hydrolytic degradation did not result in such a peak up to day 28. This peak could theoretically originate from free carboxylic acid groups (-COOH) or ester moieties [22]. The former case would be attributed to the enhanced cleavage of

esters or amide bonds, leading to formation of –COOH terminated chains, which is expected. The latter case, i.e. emergence of ester peak under oxidative and Collagenase degradation, may not have been expected under the applied conditions. One possible explanation is the increased concentration of ester groups in the degraded hydrogel owing to increased degradation of other moieties, particularly amide bonds or polypeptides.

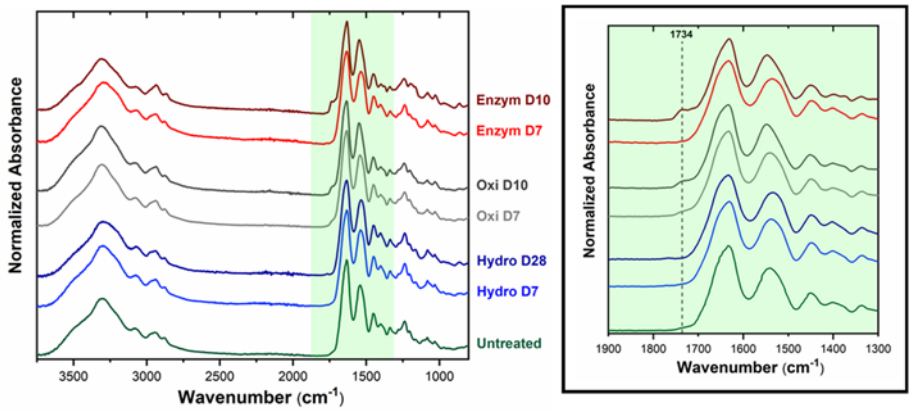


Figure 4: FTIR spectra of freeze-dried samples following partial degradation in degradation media simulating in hydrolytic, oxidative and enzymatic degradation conditions at different time points. Right graph in box represents an enlargement between 1900-1300 $cm^{-1}$.

Considering possible reactions during synthesis of the hydrogel, the hydrogel network mainly contains urea linkages from reaction between isocyanate and amine groups during reaction of LDI and gelatin, ester groups from the ethyl ester moieties from LDI molecule, alongside amide bonds naturally occurring in gelatin [19]. Conceptually, in the case of hydrolytic degradation, ester groups are most susceptible to hydrolysis, followed by amide and urea due to increasing mesomeric stabilization leading to enhanced stability [23]. Hence, we postulate that hydrolytic degradation resulted in some cleavage of ester bonds in comparison to the amide-based backbone and urea-based linkages in the investigated hydrogel, leading to the slight decrease in mass loss and rheological properties. Hydrolysis of the ethyl ester group would lead to formation of ethanol and carboxyl group terminated moiety.

In the investigated hydrogels, we suggest that oxidative degradation occurred predominantly at the polypeptide bonds and possibly the urea linkages [12], leading to degradation of the hydrogel backbone structure. Indeed, oxidative degradation occurred rapidly with loss of integrity and mechanical properties G' and G" in the investigated hydrogels. As ester groups possess stronger resistance against oxidative degradation [12], an increased concentration of ester groups relative to other functional moieties in the remaining samples may be possible, which may have led to its detection under FTIR. Under oxidative conditions, lysine, alongside proline and arginine which are also present in gelatin, have been shown be prone to abstraction of its α-hydrogen by hydroxyl radicals, which initiates chain scission leading to formation of small molecules including $\alpha$-ketoacids, carbon dioxide, ammonium ions, oximes and carboxylic acids [24, 25]. Considering that these processes and products are native within the physiological environment, the toxicity concerns for application of the investigated hydrogel as a degradable implant remains low.

Collagenase I has also been proven to rapidly degrade non-crosslinked gelatin within 12 hours [18], along with a range of crosslinked gelatin material [26], hence indicating capability of Collagenase in cleaving the polypeptide backbone in gelatin. Urea linkages, on the other hand, were shown to be relatively resistant against Collagenase I [27, 28]. In the investigated hydrogel, the dominant degradation would be cleavage of polypeptide backbone of gelatin, also evidenced by the rapid mass loss and mechanical properties G' and G". In all cases, the postulations here require information from further chemical analysis to identify the actual nature of the degradation mechanism and products.

In another type of gelatin hydrogel reacted with hexamethylene-diisocyanate after electrospinning, Kishan *et al.* reported complete mass loss in 0.02 U/mL Collagenase I on day 10-35 depending on the crosslinker ratio [18]. The results are within a comparable range to the degradation rate of the hydrogels in our present study. An earlier *in vivo* study of our hydrogels in the form of non-porous film reported complete degradation within 63 days in dorsal skin pockets in mice [8], which is a timeframe longer than the 21 days under the simulated oxidative and enzymatic degradation recorded in this study. This difference can be attributed to the porosity of the hydrogel in the present study, which allowed higher contacting surface area with degradation media leading to faster degradation. Other possible influential factors may include different hydrogel dimensions, the animal model and implantation site selected, as well as the actual presence and concentration of ROS or enzymes over time at the site of implantation, which illustrates the complexity of translation from *in vitro* to *in vivo* situation. Nonetheless, the present *in vitro* study illustrating individual contributions of different degradation mechanisms may serve as basis to better understand the interplay among the different factors in the *in vivo* environment.

## CONCLUSION

Hydrogels from gelatin and LDI are hydrolytically relatively stable, but are susceptible to degradation by oxidation or Collagenase I. The advantages of such degradation features are its stability over wet production procedures, long-term storage as sterilized material, and handling prior to surgical implantation, while being degradable *in vivo* upon implantation. The foreseeable degradation products, including polypeptide residues from gelatin, amino acids such as lysine and its associated small molecule break-down products, carbon dioxide and ethanol, possess low toxicity concerns. Importantly, understanding the degradation kinetics and chemistry is not only useful for determination of degradation products to ensure tissue compatibility and patient safety, but can also lead to potential fine-tuning of degradation kinetics of next-generation biomaterials.

## ACKNOWLEDGEMENT

The work was financially supported by the Helmholtz-Association through programme-oriented funding and by the Federal Ministry of Education and Research, Germany through the Programme Health Research (Grant No. 13GW0098). The authors also like to thank Regine Apostel, Monique Hannemann, Nicole Schneider and Andrea Pfeiffer for technical assistance in hydrogel synthesis and characterization.

## References


1. A. S. Mao and D. J. Mooney, *Proc Natl Acad Sci U S A* **112** (47), 14452-14459 (2015).
2. K. Sadtler, A. Singh, M. T. Wolf, X. Wang, D. M. Pardoll and J. H. Elisseeff, *Nat Rev Mat* **1** (7), 16040 (2016).
3. D. F. Williams, *Front Bioeng Biotechnol* **7**, 127 (2019).
4. Z. Bao, C. Xian, Q. Yuan, G. Liu and J. Wu, *Adv Healthc Mater* **8**, 1900670 (2019).
5. K. Su and C. Wang, *Biotechnol Lett* **37** (11), 2139-2145 (2015).
6. A. T. Neffe, B. F. Pierce, G. Tronci, N. Ma, E. Pittermann, T. Gebauer, O. Frank, M. Schossig, X. Xu, B. M. Willie, M. Forner, A. Ellinghaus, J. Lienau, G. N. Duda and A. Lendlein, *Adv Mater* **27** (10), 1738-1744 (2015).
7. J.-Y. Zhang, E. J. Beckman, J. Hu, G.-G. Yang, S. Agarwal and J. O. Hollinger, *Tiss Eng* **8** (5), 771-785 (2002).
8. C. Tondera, S. Hauser, A. Kruger-Genge, F. Jung, A. T. Neffe, A. Lendlein, R. Klopfleisch, J. Steinbach, C. Neuber and J. Pietzsch, *Theranostics* **6** (12), 2114-2128 (2016).
9. A. C. Weems, K. T. Wacker, J. K. Carrow, A. J. Boyle and D. J. Maitland, *Acta Biomater* **59**, 33-44 (2017).
10. M. A. Schubert, M. J. Wiggins, J. M. Anderson and A. Hiltner, *J Biomed Mater Res* **34** (4), 519-530 (1997).
11. J. R. Martin, M. K. Gupta, J. M. Page, F. Yu, J. M. Davidson, S. A. Guelcher and C. L. Duvall, *Biomaterials* **35** (12), 3766-3776 (2014).
12. M. C. P. Brugmans, S. H. M. Sntjens, M. A. J. Cox, A. Nandakumar, A. W. Bosman, T. Mes, H. M. Janssen, C. V. C. Bouten, F. P. T. Baaijens and A. Driessen-Mol, *Acta Biomater* **27**, 21-31 (2015).
13. M. A. Schubert, M. J. Wiggins, M. P. Schaefer, A. Hiltner and J. M. Anderson, *J Biomed Mater Res* **29** (3), 337-347 (1995).
14. D. K. Dempsey, C. Carranza, C. P. Chawla, P. Gray, J. H. Eoh, S. Cereceres and E. M. Cosgriff-Hernandez, *J Biomed Mater Res A* **102** (10), 3649-3665 (2014).
15. Y. Lee, J. W. Bae, J. W. Lee, W. Suh and K. D. Park, *J. Mater. Chem. B* **2** (44), 7712-7718 (2014).
16. ISO 10993-13:2010 Biological evaluation of medical devices — Part 13: Identification and quantification of degradation products from polymeric medical devices.
17. H. M. Wang, Y. T. Chou, Z. H. Wen, C. Z. Wang, C. H. Chen and M. L. Ho, *PLoS One* **8** (6), e56330 (2013).
18. A. P. Kishan, R. M. Nezarati, C. M. Radzicki, A. L. Renfro, J. L. Robinson, M. E. Whitely and E. M. Cosgriff-Hernandez, *J Mater Chem B* **3** (40), 7930-7938 (2015).
19. G. Tronci, A. T. Neffe, B. F. Pierce and A. Lendlein, *J Mater Chem* **20** (40), 8875-8884 (2010).
20. S. P. Zustiak and J. B. Leach, *Biomacromolecules* **11** (5), 1348-1357 (2010).
21. E. Delebecq, J. P. Pascault, B. Boutevin and F. Ganachaud, *Chem Rev* **113** (1), 80-118 (2013).
22. G. Socrates, *Infrared and Raman characteristic group frequencies: tables and charts*, 3rd ed. (John Wiley & Sons, 2001).
23. B. Kallies and R. Mitzner, *J Mol Model* **4** (6), 183-196 (1998).
24. A. E. Hafeman, K. J. Zienkiewicz, A. L. Zachman, H. J. Sung, L. B. Nanney, J. M. Davidson and S. A. Guelcher, *Biomaterials* **32** (2), 419-429 (2011).
25. E. R. Stadtman, *Ann Rev Biochem* **62** (1), 797-821 (1993).
26. G. Yang, Z. Xiao, H. Long, K. Ma, J. Zhang, X. Ren and J. Zhang, *Sci Rep* **8** (1), 1616 (2018).
27. N. A. Sears, G. Pena-Galea, S. N. Cereceres and E. Cosgriff-Hernandez, *J Tissue Eng* **7**, 1-9 (2016).
28. H. L. Fu, Y. Hong, S. R. Little and W. R. Wagner, *Biomacromolecules* **15** (8), 2924-2932 (2014).